ROME 2008
LEVERAGING TECHNOLOGY

Applying geostatistical filtering techniques to near-surface geophysics: two examples for refraction surveying and gravimetry

Jeannée Nicolas (1), Mari Jean-Luc (2)

(1) Géovariances, Avon, France
(2) Institut Français du Pétrole, IFP school, Rueil-Malmaison, France
e-mail: jeannee@geovariances.fr- jean-luc.mari@ifp.fr

Abstract

Geostatistical filtering techniques are commonly applied to improve the quality of seismic data such as velocity cubes or interpreted horizons. However, to our knowledge their application to near-surface geophysics is quite new. The present paper therefore aims at illustrating the benefit of these techniques through two examples. In the first one, dedicated to refraction imaging, geostatistics allow to filter out acquisition artifacts and to identify main geological features. The second example presents how a global trend can be filtered out in a Bouger's anomaly dataset (gravimetry context), therefore letting appear local anomalies that are of interest.

Firstly, principles of geostatistical filtering techniques are briefly recalled. Then the two examples and the added value of geostatistics are presented.

Introduction

Geostatistical filtering techniques are commonly applied to improve the quality of seismic data such as velocity cubes or interpreted horizons. However, to our knowledge their application to near-surface geophysics is less common. Firstly, principles of geostatistical filtering techniques are briefly recalled. Then it is shown how geostatistical filtering can be used to decompose "geophysical anomalies" into long and short wavelength components.

The added value of geostatistics is presented with two field examples. In the first one, dedicated to refraction surveying, geostatistics allow to filter out acquisition artifacts and to identify the main geological features. The second example presents how a global trend can be filtered out in a Bouguer anomaly dataset (gravity context), letting appear interesting local anomalies.

Geostatistical filtering techniques

Geostatistics is commonly applied to study the spatial variability of seismic datasets and to detect footprints due to the acquisition procedure (Dubrule, 2003). Their use relies on a two-step procedure. Firstly, variogram modeling consists in fitting analytical models defined by a few parameters (range, sill, nugget effect) to the experimental variograms computed from the input data. Then, several filtering techniques can be applied, relying on the previous variogram model. Geostatistical filtering cover several methods: kriging analysis, factorial kriging and to some extent drift estimation (Matheron, 1982; Chilès and Delfiner, 1999).

The underlying assumption is that the variable of interest, *Z(x)*, can be decomposed in several components

$$Z(x) = Y_1(x) + ... + Y_n(x) + m(x)$$

where the $Y_i(x)$ $(i = 1, \ldots, n)$ correspond to stationary and uncorrelated components of the phenomenon and *m(x)* represents the unknown mean (large scale trend). Once a variogram model is fitted, the efficiency of the filtering technique depends on the ability to interpret each variogram structure in terms of spatial component. For instance, in the refraction example, the variogram will be fitted by a model constituted of 5 components:

$$\gamma(h) = c_0 + \gamma_{aa}(h) + \gamma_{gh}(h) + \gamma_{gf1}(h) + \gamma_{gf2}(h)$$

with:

- c_0 a nugget effect, interpreted as random acquisition noise,
- $\gamma_{aa}(h)$ an anisotropic spherical short range component in the crossline direction due to acquisition artifacts,
- $\gamma_{gh}(h)$ a mid-range cubic structure corresponding to geological heterogeneities,
- $\gamma_{gf1}(h)$ and $\gamma_{gf2}(h)$ two long-range structures corresponding to long wavelength geological features.

Strictly speaking, factorial kriging consists in estimating, knowing the original data $Z(x_i)$ and the variogram model, one particular component $Y_i(x)$ (zero-mean). From a kriging system point of view, factorial kriging only requires a slight modification of the right-hand side term, keeping only the variogram component corresponding to the target $Y_i(x)$. It is sometimes convenient to present things in a slightly different way, particularly if one aims at filtering out one component (for instance acquisition noise) instead of estimating one particular component. In this case, the kriging system is solved with, in the right-hand side term, the entire variogram model except the component to be filtered out.

Finally, the trend *m(x)* may sometimes be modeled by a simple polynomial expression:

$$m(x) = \sum_l a_l f^l(x)$$

where the $f^l(x)$ are usually monomials of the coordinates and the a_l are unknown fixed (or at least smoothly varying) coefficients. Note that in general: (i) there is no optimal way to

separate *m(x)* and the residuals $Y(x) = Z(x) - m(x)$, and (ii) the decomposition is relevant for a particular scale of observation. Universal kriging provides an estimate of Z for this model, without having to estimate the trend itself. However, when estimating this trend is precisely the goal, the latter can be obtained directly from the universal kriging system (written in covariances) by just equating to zero its right-hand side term. The residual component $Y(x)$ can be obtained by subtracting the estimated mean from the estimate of the variable itself: $Y^*(x) = Z^*(x) - m^*(x)$ or by filtering directly the drift component; both approaches are equivalent because of the linearity of the kriging system. This universal kriging approach will be illustrated on the gravimetry example.

One noticeable application of factorial kriging to gravimetry is presented in Chilès and Guillen (1984). In particular, the authors compare the factorial kriging approach with a spectral analysis. Whereas the latter requires a preliminary interpolation on a regular grid, the factorial kriging approach has the advantage of performing both the filtering and the smoothing in one step.

First example: Refraction surveying

The dataset comes from the Experimental Hydrogeological Site (EHS), located near Poitiers city (France). The concerned aquifer consists of tight karstic Jurassic carbonates of about 100 m in thickness beneath a weathering zone of Tertiary clays.

Refraction seismic surveying, described in detail by Mari and Porel (2007), has been used to map the irregular shape of the top of karstic reservoir (Figure 1, top left).

The experimental variogram, computed in the main directions of continuity (in line and cross line directions) has been modeled by several nested structures: a small nugget effect (random noise), a cubic structure with a range equal to 50m, consistent with the size of the geological heterogeneities, two spherical structures with ranges equal to 100m and 400m. The cross-line variogram presents an additional variability source, attributable to acquisition artifacts. This component is modeled by a spherical basic structure with a range equal to 5m. The nugget effect and the small scale spherical model (5m in the crossline direction), which have no physical meaning and are due to acquisition artifacts, are filtered out during the interpolation process by factorial kriging (Figure 1, top right).

By comparison with the original dataset, the interpolated map allowed to identify an erroneous acquisition line, responsible for the additional variability component in the cross line direction. After the removal of this line, an omnidirectional variogram is computed on the updated dataset (Figure 1, bottom left), being mostly interested by the small scale variability, up to 50-75m. The resulting variogram model is constituted by a nugget effect, a cubic structure with range 55m and a long scale spherical structure with range 145m.The final WZ map is obtained using kriging, with filtering of the nugget effect (random acquisition noise) and small scale structure (cubic 55m) in order to obtain a map which makes appear the large scale structures. Figure 1 (bottom right) shows the resulting weathering depth map. The map enables to identify the directions of the geological structures at the scale of the map: the azimuth of the main structure is N90.

Second example: Bouguer anomaly

The gravimetric data were gathered by the Geophysical Institute, University of Lausanne, under the direction of Professor Raymond Olivier (Atlas gravimétrique de la Suisse au 1/10000). The area of Aubonne is located between Geneva and Lausanne in Switzerland. The geology of this area consists in a Molasse basement (Chattien sandstone) dug with furrows filled by quaternary sediments. The Bouguer model is computed using the 1967 Ellipsoïde and the model density is 2.4. This density corresponds to the Molassic basement. The topographic correction has been applied up to 167 km (Olivier and Simard, 1981).

Firstly, the raw Bouguer anomaly has been interpolated (100m x 100m) using universal kriging (Figure 2 top left). Variogram analysis (Fig.2 top right) has been performed on data residuals after the removal of a global linear trend on both coordinates. Geostatistical filtering

has been used to decompose the Bouguer anomaly into a long wavelength structure (regional anomaly, corresponding to the global trend, Fig. 2 bottom left) and a short wavelength structure (residual anomaly, Fig. 2 bottom right). On the residual Bouguer anomaly map, one can clearly see a negative anomaly oriented North West – South East. It points out a furrow in the bed rock. A borehole, drilled at 522.3/150.4, has given a depth of 146m.

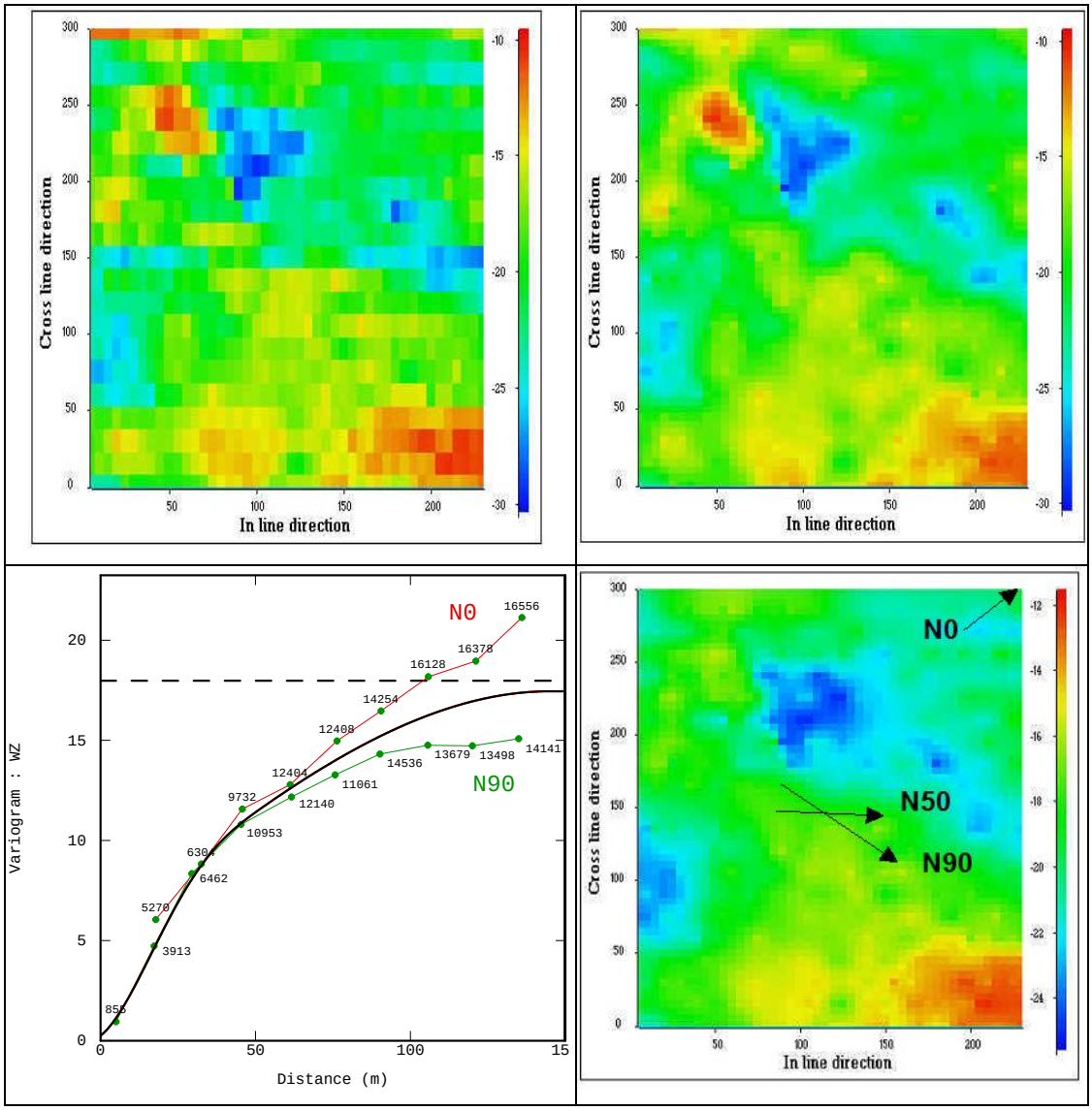

Figure 1: Refraction survey : detection of long wavelength anomaly. Top left: raw depth map (5m x 15m) of the weathering zone. Top right: WZ depth map obtained by factorial kriging on the raw dataset (5m x 5m). Bottom left: Experimental directional variograms and modeled omnidirectional variogram, aftet the removal of an erroneous line. Bottom right: weathering depth map once filtered the small scale structures, orientation of the geological structures.

Conclusion

The aim of this work is to demonstrate how variogram analysis and geostatistical filtering can be used to detect and filter both random acquisition noise and foot prints in near-surface geophysics. It also illustrates how geostatistical filtering techniques can be used to decompose "geophysical anomalies" and identify target geological features.

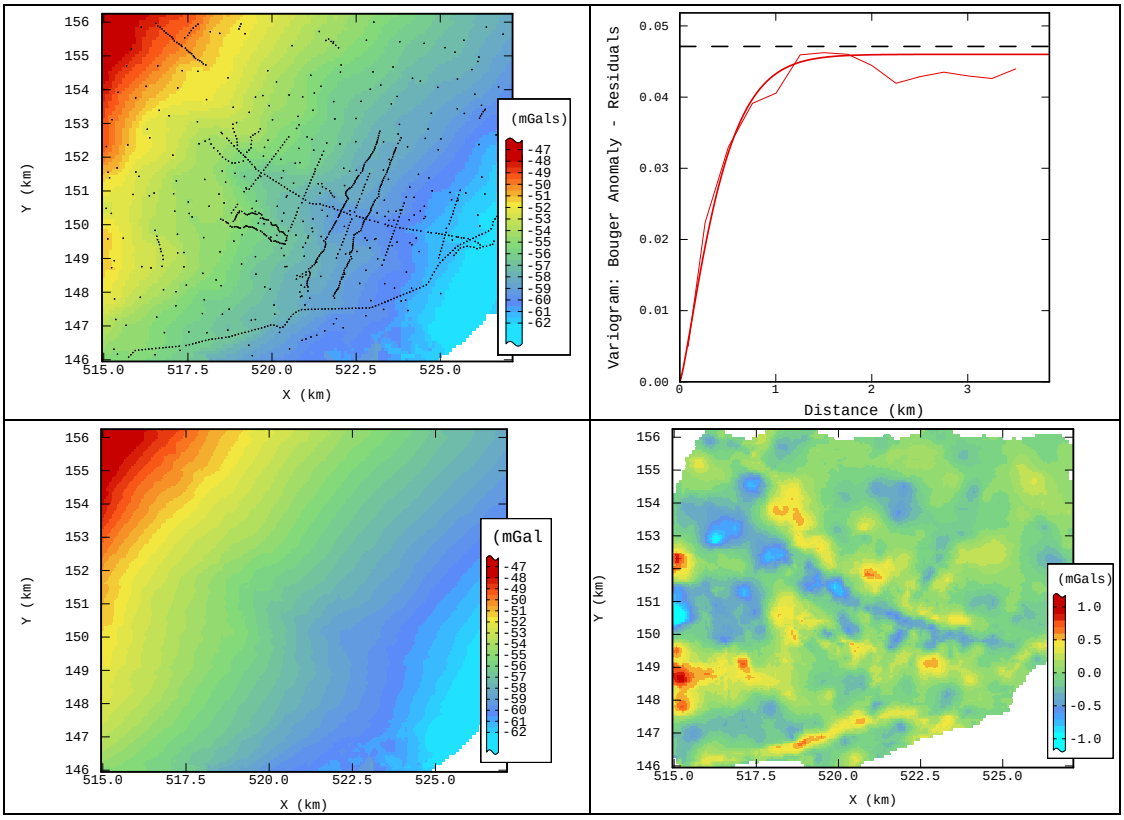

Figure 2: Detection of a furrow on a Bouguer anomaly dataset. Top left: raw data locations (black dots) and interpolated map (universal kriging). Top right: experimental (thin line) and modeled (bold) variogram. Bottom left: regional Bouguer anomaly obtained by kriging of the global trend. Bottom right: residual Bouguer anomaly after the removal of the global trend.

Acknowledgements

We thank University of Poitiers and IFP for the permission to use the refraction data recorded on The Poitiers hydrogeological site. We thank Raymond Olivier and Institut Geophysique de Lausanne for the permission to present the Aubonne gravity dataset. We are grateful to Dominique Chapellier for providing useful information and help on gravity processing. Geostatistical results are obtained with ISATIS® software (Geovariances, 2007).

References

Chilès J.P. and Guillen A. [1984] Variogrammes et krigeages pour la gravimétrie et le magnétisme. *Sciences de la Terre, Série Informatique Géologique*, **20**, 455-468.

Chilès J.P. and Delfiner P. [1999] *Geostatistics modeling spatial incertainty*. Wiley series in probability and statistics.

Dubrule O. [2003] 2003 Distinguished Instructor Short Course – Distinguished Instructor series, N°6, SEG & EAGE.

Geovariances [2007] *ISATIS technical references*. Geovariances & Ecole des Mines de Paris, version 7.0, 138 p.

Mari J.L and Porel, G. [2007] 3D seismic imaging of a near–surface heterogeneous aquifer: a case study. *Oil & Gas Science and Technology*, Rev IFP, DOI: 10.2516/ogst:2007077.

Matheron G. [1982] Pour une analyse krigeante des données régionalisées. Internal report N-732, Centre de Géostatistique et de Morphologie Mathématique, Ecole des Mines de Paris, Janvier 1982.

Olivier R.J. and Simard R.G. [1981] Improvement of the conic prism model for terrain correction in rugged topography. *Geophysics*, **46**(7), 1054-1056.